# Transverse Momentum Spectra of Pions in Particle and Nuclear Collisions and Some Ratio-Behaviours: Towards A Combinational Approach

# Bhaskar De†§, S. Bhattacharyya†|| and P. Guptaroy‡

- † Physics and Applied Mathematics Unit(PAMU), Indian Statistical Institute, Kolkata 700108, India.
- ‡ Department of Physics, Raghunathpur College, Raghunathpur 723133, Purulia (WB), India.

Abstract. The nature of transverse momentum dependence of the inclusive cross-sections for secondary pions produced in high energy hadronic (PP), hadronuclear (PA) and nuclear (AA) collisions has here been exhaustively investigated for a varied range of interactions in a unified way with the help of a master formula. This formula evolved from a new combination of the basic Hagedorn's model for particle (pion) production in PP scattering at ISR range of energies, a phenomenological approach proposed by Peitzmann for converting the results of NN(PP) reactions to those for either PA or AA collisions, and a specific form of parametrization for mass number-dependence of the nuclear cross sections. This grand combination of models (GCM) is then applied to analyse the assorted extensive data on various high energy collisions. The nature of qualitative agreement between measurements and calculations on both the inclusive cross-sections for production of pions, and some ratios of them as well, is quite satisfactory. The modest successes that we achieve here in dealing with the massive data-sets are somewhat encouraging in view of the diversity of the reactions and the very wide range of interaction energies.

 $\mathbf{Keywords}\;:\;$  Inclusive Cross-sections, Heavy Ion Collisions.

PACS numbers: 13.60.Hb, 25.75.-q, 25.40.Ve.

Submitted to: J. Phys. G: Nucl. Phys.

### 1. Introduction

The nature of transverse momentum spectra of the secondaries produced in various high energy nuclear and particle collisions[1, 2, 3, 4, 5, 6] is still of much importance and interest for some various well-known reasons. Pions constitute the most abundant variety among the various secondaries produced in high energy collisions which include particle-particle, particle-nucleus and nucleus-nucleus interactions. Within the confine of the present work, the word 'particle' refers mainly to proton, because no other hadron, as either projectile or target, has here been reckoned with. In this work we would concentrate on analyzing the nature of transverse momentum dependence of the inclusive pion production cross section for some high energy nucleon- and nucleus-induced reactions and also on understanding the characteristics of some of the cross section-ratio versus transverse  $momentum(p_T)$  plots. This indicates certainly no preferential treatment to  $p_T$ -spectra as such; rather it is because of the fact that the rapidity spectra of pions have already been studied with an identical approach, and the encouraging results of our investigation have been communicated in a separate work[7]. The ratiobehaviours are significant, mainly because of the fact that they offer a dependable consistency check-up of the final working formula which has here been framed and forwarded mostly from the phenomenological points of view; and which has also finally been put into use for actual calculations of the results. Besides, comparing the results obtained by the model of our choice with some of the existing and the most prominent models would also be one of our objectives here. Still, trying to obtain first reliably good fits to the data on inclusive cross sections versus transverse momenta  $(p_T)$  values of the pions produced in NN, NA, and AA interactions from a very generalized approach constitutes here our topmost concern and priority in this work.

Regarding the very basic motivations of this work, we offer precisely the following few points: (i) The high energy physicists (both theorists and experimentalists) have, by and large, focused heavily on  $m_T$ -scaling behaviour put forward by Hagedorn for PP collision in his statistical model[8]. But for production of particles at relatively high transverse momenta the  $m_T$ -scaling hypothesis is seen to be experimentally inapplicable for which Hagedorn himself later shifted to a power law form[9] of expression which would be used in the present work. The universal function in the Hagedorn model with  $m_T$ -scaling is a Bose-Einstein or Fermi Dirac distribution and depends on a simple parameter, i.e., the slope parameter. Contrary to this picture we would try to attack the problem in reverse and try to determine the universal behaviour with no particular concern about the status of  $m_T$ -scaling by analysing intensively and extensively the experimental data on both the nucleon-nucleon (PP) and nucleon (nucleus)-nucleus interactions. This aspect is unique in our approach. (ii) Secondly, we have attempted to show somewhat clearly the degree of dependence of AA collisions on PP collisions and also the extent of intertwining between proton-proton and nucleus-nucleus reactions. In fact, the entire energy-dependence of particle production characteristics of nucleus-nucleus collisions has here been transmuted to the case of proton-proton reaction at the same center of mass energy. This has helped us to construct a pathway between NN and NA/AA interactions. (iii) Thirdly, our approach to the analysis of the problem is not based on any apriori assumptions of the standard and textual premises of the QGP hypotheses or about the constituent picture of any of the popular brand of theories.

The organization of this paper is as follows. In the next section (Section 2) we give the outline of the basic outlook and the approach to be taken up for this study. In Section 3 we present the essential steps in the methodology of our work here. The Section 4 contains the results of model-based calculations and some broad discussion on the results obtained by this combinational approach. In Section 5 we have made a comparison of the results obtained by the model of our choice and those by some other very front-ranking ones. The last section is reserved for summing up the conclusions and making some points of observational interest and general validity.

# 2. The Basic Approach: Tracing the Outline

Following the suggestion of Faessler[10] and the work of Peitzmann[11] and also of Schmidt and Schukraft[12], we propose here a generalized empirical relationship between the inclusive cross-section for pion production in nucleon(N)-nucleon(N) collision and that for nucleus(A)-nucleus(A) collision as given below:

$$E\frac{d^3\sigma}{dp^3} (AB \to \pi X) \sim (A.B)^{\phi(y, p_T)} E\frac{d^3\sigma}{dp^3} (PP \to \pi X) , \qquad (1)$$

where  $\phi(y, p_T)$  could be expressed in the factorization form,  $\phi(y, p_T) = f(y) g(p_t)$ .

While investigating a specific nature of dependence of the two variables  $(y \text{ and } p_T)$  either one of these is assumed to remain constant. In other words, more particularly, if and when the  $p_t$ -dependence is studied by experimental groups, the rapidity factor is treated to be constant and the vice-versa. So, the formula turns into

$$E\frac{d^3\sigma}{dp^3} (AB \to \pi X) \sim (A.B)^{g(p_T)} E\frac{d^3\sigma}{dp^3} (PP \to \pi X) , \qquad (2)$$

The main bulk of work, thus, converges to the making of an appropriate choice of form for  $g(p_T)$ . And the necessary choices are to be made on the basis of certain premises and physical considerations which do not violate the canons of high energy particle interactions.

The expression for inclusive cross-section of pions in proton-proton/antiproton scattering(see figures 1 and 2) at high energies in Eqn.(2) could be chosen in the form suggested first by Hagedorn[9]:

$$E\frac{d^3\sigma}{dp^3} (PP \to \pi X) = C_1 \left(1 + \frac{p_T}{p_0}\right)^{-n},$$
 (3)

where  $C_1$  is the normalization constant, and  $p_o$ , n are interaction-dependent chosen phenomenological parameters for which the values are to be obtained by the method of fitting. Their  $\sqrt{s}$ -dependences are here proposed to be given by the following formulations:

$$p_0(\sqrt{s}) = a + \frac{b}{\sqrt{s} \ln(\sqrt{s})} \tag{4}$$

where a = 1.5, b = 79.4 and

$$n(\sqrt{s}) = \acute{a} + \frac{\acute{b}}{\ln^2(\sqrt{s})} \tag{5}$$

with a=6.5, b=127. The  $\sqrt{s}$ -dependence of  $p_0$  and n would be shown later diagrammatically in the text and their data-base would also be indicated. The nature and significance of these parameters could be appreciated from the work of Hagedorn[9], and those of Bielich et al[13] and Albrecht et al[14]. The ratio  $p_0/n$  characterizes the intercept of the slope of the transverse momentum spectra in the limit  $p_T \to 0$  and has a value near 150 MeV for PP and also for some nuclear collisions. The prescribed limit of its value is 130-170 MeV which we have shown to be correct and consistent in our work.

The final working formula for the nucleus-nucleus collisions is now being proposed here in the form given below:

$$E\frac{d^3\sigma}{dp^3} (AB \to \pi X) \approx C_2 (A.B)^{(\epsilon + \alpha p_T - \beta p_T^2)} E\frac{d^3\sigma}{dp^3} (PP \to \pi X) , \qquad (6)$$

with  $g(p_T) = (\epsilon + \alpha p_T - \beta p_T^2)$ . This quadratic parametrization is our own suggestion and is called De-Bhattacharyya parametrization(DBP). In the above expression  $C_2$  is the normalization term which has a dependence either on the rapidity or on the rapidity density of the pion;  $\epsilon$ ,  $\alpha$  and  $\beta$  are constants for a specific set of projectile and target.

Earlier works [14, 15, 16] showed that  $g(p_T)$  is less than unity in the  $p_T$ -domain,  $p_T < 1.5 \text{ GeV/c}$ . Besides, it was also observed that the parameter  $\epsilon$ , which gives the value of  $g(p_T)$  at  $p_T = 0$ , is also less than one and this value differs from collision to collision. The other two parameters  $\alpha$  and  $\beta$  essentially determine the nature of curvature of  $g(p_T)$ . However, in the present context precise determination of  $\epsilon$  is not possible for the following understated reasons:

(i) To make our point let us recast the expression for (6) in the form given below:

$$E\frac{d^3\sigma}{dp^3}(AB \to \pi X) \approx C_2 (A.B)^{\epsilon} (A.B)^{(\alpha p_T - \beta p_T^2)} (1 + \frac{p_T}{p_0})^{-n}$$
 (7)

Quite obviously, we have adopted here the method of fitting. Now, in Eqn.(7) one finds that there are two constant terms  $C_2$  and  $\epsilon$  which are neither the coefficients nor the exponent terms of any function of the variable,  $p_T$ . And as  $\epsilon$  is a constant for a specific collision at a specific energy, the product of the two terms  $C_2$  and  $(A.B)^{\epsilon}$  appears as just a new constant. And, it is quite difficult to obtain fit-values simultaneously for two constants of the above types through the method of fitting.

(ii) From Eqn.(2) the nature of  $g(p_T)$  can easily be determined by calculating the ratio of the logarithm of the ratios of nuclear-to-PP collision and the logarithm of the product AB. Thus, one can measure  $\epsilon$  from

the intercept of  $g(p_T)$  along y-axis as soon as one gets the values of  $E\frac{d^3\sigma}{dp^3}$  for both AB collision and PP collision at the same c.m. energy. In the present study we have tried to consider the various collision systems in as many number as possible. To do so, we have to consider the data on normalized versions of  $E\frac{d^3\sigma}{dp^3}$  for many collision systems for which clear  $E\frac{d^3\sigma}{dp^3}$ -data were not available to us. Furthermore, from these normalized versions we can/could not extract the appropriate values of  $E\frac{d^3\sigma}{dp^3}$  as the normalization terms, total inclusive cross-sections( $\sigma_{in}$ ) etc., for these collision systems cannot always be readily obtained. Besides, it will also not be possible to get readily the data on inclusive spectra for PP collisions at all c.m.energies, like e.g., at  $\sqrt{s} = 17.8 GeV$ (c.m. energy of Pb + Pb collision).

In order to sidetrack these difficulties and also as an escape-route, we have concentrated almost wholly to the values of  $\alpha$  and  $\beta$  for various collision systems and the effect of  $C_2$  and  $\epsilon$  has been combined into a single constant term  $C_3$ . Hence, the final expression becomes,

$$E\frac{d^3\sigma}{dp^3}(AB \to \pi X) \approx C_3 (A.B)^{(\alpha p_T - \beta p_T^2)} (1 + \frac{p_T}{p_0})^{-n}$$
 (8)

with  $C_3 = C_2(A.B)^{\epsilon}$ .

The exponent factor term  $\alpha p_T - \beta p_T^2$  obviously represents here  $[g(p_T) - \epsilon]$  instead of  $g(p_T)$  alone. Thus, after obtaining fit-values of  $\alpha$  and  $\beta$ , if  $[g(p_T) - \epsilon]$  are plotted for various collision systems, all the curves would originate from a single point, i.e. origin; and the systems and processes are then really comparable. In other words, in this convenient way we could study and check the scaling characteristics of  $g(p_T)$  with respect to the collision systems.

The expression(8) given above is the physical embodiment of what we have termed to be the grand combination of  $\operatorname{models}(\operatorname{GCM})$  that has been utilized here. The results of PP scattering are obtained in the above on the basis of eqn.(3) provided by Hagedorn's  $\operatorname{model}(\operatorname{HM})$ ; and the route for converting the results of NN to NA or AB collisions is built up by the Peitzmann's approach(PA) represented by expression(2). The further input is the De-Bhattacharyya parametrization for the nature of the exponent. Thus, the GCM is the totality and resultant of HM, PA and the DBP, all of which are used here.

#### 3. The Procedure

At the very start let us mention a few points of special concern. Though pions are produced in all three varieties in the physical processes, we have treated their cases here in an average and charge-independent way. Secondly, we treated theoretically the PP and  $P\bar{P}$  reactions at accelerator or collider energies on an equivalent footing, as annihilation channels are found to have no or negligible contributions at high energies,  $\sqrt{s} \ge 10$  GeV. Besides, while collecting data-sets we have, at times, assumed and used the total negative particle multiplicity to be physically equivalent to negative pion multiplicity for all practical purposes, as the pions are overwhelmingly predominant in number compared to all other particle-species. And this is done only under compulsion arising out of the non-availability of direct and reliable data on pion production in the relevant collision.

The first step towards progress in the present work consists of fitting the inclusive transverse momentum cross sections of pions produced in both PP and  $P\bar{P}$  collisions available at various high energies with the help of the proposed form given in Eqn.(3). The values of  $p_0$  and n at different high energies are specifically noted in Table 1 and Table 2 for the case of pion production alone. Next, we draw graphs to investigate closely the nature of  $\sqrt{s}$ -dependence of these two model-based parameters, viz,  $p_0$  and n. The plots of  $p_0$  vs.  $\sqrt{s}$  and n vs.  $\sqrt{s}$  are presented in Fig.3. While plotting graphs we have obviously assumed that at very high energies the proton-proton and proton-antiproton collisions could be treated at par and with the acceptance of equivalence between each other.

Hereafter, in studying the nature of  $p_T$ -spectra in all nucleon-nucleus and nucleus-nucleus collisions, the interaction energy in all cases of nucleus-induced reactions is invariably converted first into the c.m. system values, that is expressed in  $\sqrt{s_{\rm NN}}$ , then the values of  $p_0$  and n are picked up from the already drawn graphical plot shown by Fig.3. While analyzing nucleus-dependence with expression(8) and trying with the fit parameters  $C_3$ ,  $\alpha$  and  $\beta$ , we have inserted these extracted values of  $p_0$  and  $p_0$  for  $p_0$  cross section term occurring in the expression(8) given above. The values of  $C_3$ ,  $\alpha$ ,  $\beta$ ,  $\chi^2$ /ndf and some other relevant information on the specifities for various nucleon-nucleus and nucleus-nucleus collisions are depicted in tabular form [Table-3]. The solid curves in all the diagrams represent the theoretical calculations. The fits, in most cases, are done within the  $p_T$ -band  $0.8 \le p_T \le 3.0 \text{ GeV/c}$ . And this choice is obviously attuned to the availability of the experimental

data in the several nuclear collisions. However, only exceptions are the cases of DD and  $\alpha\alpha$  interactions at  $E_{Lab} = 480 A$  GeV where the  $p_T$ -ranges are much wider. And this would be evident from the Fig.5. The ratio values are calculated simply by dividing the valid expression(8) for the corresponding collisions between any pair of projectile and target with some multiplicative factors shown in the several ratio-figures. No further complications about them are taken here into account.

## 4. Model-Based Results and Discussions

Taking the cue from the preceding section one might state that the actual start of the present work takes place from plotting of the  $p_0$  vs.  $\sqrt{s}$  graph, and of n vs.  $\sqrt{s}$  graph(Fig.3), which offer us the necessary lever to apply the connective corridor or connector built up by Peitzmann's approach (PA) for converting the results of nucleonnucleon collision to that of nucleon-nucleus or nucleus-nucleus interaction at high energy. The total work is the combination of these two models and of the parametrization referred to as DBP. The nature of agreement here between all model-based calculations and experimental measurements is modestly fair. The reproductions of the data on invariant inclusive cross section vs. transverse momentum plots, right from the proton-deuteron collision to the heaviest lead-lead interaction, and also the data involving some Uranium-induced collisions as well, are presented in the diagrams from Fig.4 to Fig.9. The numerical values shown in the seventh column of Table 3 depict the corresponding  $\chi^2$ /ndf values which indicate the quantitative measure of the quite satisfactory nature of fits in qualitative terms, save perhaps the case of sulphur-lead reaction shown in Fig.8. Let us treat this as a minor exception for which various reasons might be at play in the various stages of measurements. But the diagrams shown in Fig.10 merit special attention. The parameters  $\alpha$  and  $\beta$  separately demonstrate a steadily flat nature at values around  $\alpha = 0.18 \pm 0.03$  and  $\beta = 0.035 \pm 0.009$  respectively with regard to the product of AB. This ensures a saturation for the penetrability of projectile into particle/parton-structure of the target nuclei. The energy  $(\sqrt{s})$ -dependence has already been inserted and there should be no double counting. Now follow some specific comments on RHIC(BNL)-spectra which claim, in recent times, a special status.

The latest stir in the field of high energy particle physics is caused by the spurt of particle production in AuAu collisions at  $\sqrt{s_{NN}} = 130$  GeV in the RHIC(BNL). We have concentrated here on the inclusive cross section of production of neutral pions in the minimum bias events[17], and also for both peripheral and central collisions [18]. The values of  $\alpha$  given in the fifth column of Table-3 for AuAu collisions do not show any appreciable change in magnitude for the three separate cases of the event-sets, while those for  $\beta$  remain same within errors. So, within the limits of  $0.8 \le p_T \le 3.0 \text{ GeV/c}$ , i.e. within the clear domain of 'soft' particle production the results on AuAu collisions at RHIC experiments modestly corroborate our claim that the parameters,  $\alpha$  and  $\beta$  are independent of the collision centrality. However, with growing values of the transverse momentum( $p_T > 3 \text{ GeV/c}$ ) i.e., for hard collision, the behaviour, in all probability, is likely to turn more complex; and initial indications to such complications are somewhat manifest by the slight but detectable deviations of the fits provided by us here for values around  $p_T > 3.5 \text{ GeV/c}$ . So, the present study does neither essentially contradict the content of Adcox et al[18], nor could essentially support the signal message received from them. Indeed, we have left aside here the measurement on average productions of charged hadron which obviously include other varieties of charged mesons and baryon-antibaryons as well. As their incorporations might spoil the exclusivity of pion production case, we have purposefully sidetracked those data in the present work; and we have converged more particularly to the transverse momentum spectra of only the neutral pions.

The features of the cross section ratios(CSR) have been displayed in the diagrams from Fig.11 to Fig.16. The plots presented in Fig.16 on prediction alone with no data are the exceptional ones. The patterns of the plots of the specific ratios versus the transverse momentum ranges are, in most cases, modestly similar with exceptions for the cases of  $\frac{\alpha+\alpha}{P+P}$ (Fig.12),  $\frac{\alpha+\alpha}{D+D}$ (Fig.12) and  $\frac{S+U}{O+U}$ (Fig.14) wherein the curvatures of both the data plots and the theoretical curves are just the opposite. But, in so far as the question of agreement between the theoretical plot versus data is concerned, there is no problem. The CSR behaviours in the two particular cases of  $\frac{\alpha+\alpha}{D+D}$ (Fig.12),  $\frac{Au+Au}{P+P}$ (Fig.16a) and  $\frac{Pb+Pb}{D+D}$ (Fig.16b) are also of obverse type, though for the former the nature of fit between theory and experiment is quite satisfactory; and for the latter two this point does not just arise as they are predictive theoretical plots. But, the question of similarity or dissimilarity between any two or among the graphs cannot be delved into in any further detail, as the data-points shown in the graphs indicate the measurements at very different energies. The actual data on predicted ratio behaviour in  $\frac{Au+Au}{P+P}$  could be obtained separately from the RHIC in future. The nature of the ratio of  $\frac{Pb+Pb}{D+D}$  could be of interest in the sense that the deuterons are the lightest known nuclei used in colliding systems and Pb is the available

heaviest nuclear species which is nowadays being frequently used as both projectile and target in the CERN SPS and will be used in future in the LHC. The dotted curves in both Fig.16(a) and Fig.16(b) indicate the range of theoretical uncertainties due to errors of averaged  $\alpha$  and  $\beta$ .

The fair agreement between the data and calculations for the ratios offers us a modestly reliable and somewhat convincing cross-check of the model for pion production in nuclear collisions that has here been proposed and developed to a certain extent.

Now, we hold the view that our analysis and results could be made far more rigorous, should the data on pion production in both PP and NA/AA interactions for different  $p_T$  in exactly the same rapidity region would be simultaneously available. But by all indications, such expectations at this stage are too unrealistic for which we have had to remain satisfied with whatever is at hand now. It is very encouraging to note that the fits reproduce data on pion production even in the not-very compatible region of rapidity in PP and AA collisions. So, it is only natural and reasonable to summarize that the same or compatible region of rapidity for both types of collisions could offer only better and much-improved fits.

# 5. The $p_T$ -Spectra in Nuclear Collision: A Brief Comparison of Some Models

Based on the analysis of the experimental data, let us mention the following few points as the summary of the main and basic features of the  $p_T$ -spectra, especially of large- $p_T$  variety, of the secondaries produced in nuclear collisions: (i) strong dependence on both target and projectile mass or mass number, (ii) very weak or no dependence on the rapidity, (iii) very weak or no dependence on the c.m.energy, (iv) dependence on impact parameter for those restricted collision wherein the full overlap of target and projectile does not occur, (v) no further  $E_T$  dependence beyond the above point. With considerations on some of these characteristics, the NA34 collaboration[19] demonstrated that the target and projectile dependence could be treated in a similar manner when parametrized by a power law of the form:

$$\frac{d\sigma}{dp_T}(P+A) = A^{\xi(p_T)} \frac{d\sigma}{dp_T}(P+P) \tag{9}$$

$$\frac{d\sigma}{dp_T}(B+A) = B^{\zeta(p_T)} \frac{d\sigma}{dp_T}(P+A) \tag{10}$$

Schmidt and Schukraft[12] pointed out how a fit of  $\xi(p_T)$  to the original Fermilab P+A data could lead to the reasonably nice description of  $\zeta(p_T)$  in a two-step manner. The similarity between  $\xi(p_T)$  and  $\zeta(p_T)$  was emphasized and was interpreted as dependence of the Cronin effect on the projectile mass number analogous to the one on the target.

Next, the WA80 Collaboration[14] made attempt to unify functionally this two-stage transitions into a single-step affair in the form of the eqn.(2) dealt with previously in Section 2. Therein the expression for  $g(p_T)$  will have to be chosen phenomenologically in such an appropriate manner as to fit the data as nicely as possible. The WA80 team proposed a simple linear form of fit for  $g(p_T)$ . in the present work we have taken a polynomial(quadratic) form instead. There is one more major difference between these two approaches. The WA80 team made choices of  $p_0$  and n values for PP and AB reactions completely separately. On the contrary we have introduced the results of  $p_0$  and n directly from our studies  $PP/P\bar{P}$  reactions at various energies. In the approach presented and pursued here the point is to find out the energy of interactions between the nuclei; and once it is known, the  $p_0$  and n values of the PP reactions at this specific energy are to be ascertained from Fig.3 and inducted in the calculations.

The performance by WA80 Collaboration[14] is essentially grounded in a sort of the physics of purturbative quantum chromodynamics(PQCD) approach in Hagedorn's form, and is also embedded in string and hydrodynamic considerations. This combination is called here the Mixed Model(MM). So, we represent the calculated results of WA80 collaboration as the product of a Mixed Model(MM). The comparison of GCM and MM with experimental data on SS and SAu reactions is given in Fig.17a. The solid lines in all the figures describe results obtained by GCM. Over the entire  $p_T$ -range the agreement with this MM is quite satisfactory; and at very high  $p_T$ -values the results based on MM have shown much better agreement than those obtained with the GCM. But there is a change in the scenario in cases of data interpretation on PbPb and PbNb cases(Fig.17a). The comparison, in this two cases, is with calculations made by Thermal Model[16] which does not show quite fair agreement with data for the region beyond  $p_T \approx 2.5 \text{ GeV/c}$ , whereas the GCM addresses competently all the measured data-points. In Fig.17(b) a comparison has been made between two sets of models on data from

AuAu collisions with two different detectors, for PbPb interaction and also for OAu reaction. And the sets of the models are (i) Modified Hydrodynamic model of Peitzmann[20] and the GCM and (ii) the PQCD-based HIJING model[21] vs. the GCM. The agreement with both data and the most popular versions of the two models could, on the whole, be rated to be modestly fair. The HIJING model is old and well-known among the Monte-Carlo simulation-based models. And, unlike the case of hydrodynamic model, there has not been any new updating of it in the recent past.

Compared to the GCM, the version of hydrodynamic model offered very recently by Peitzmann[20] provides certainly a little better agreement, especially at large values of  $p_T$ . This is observed in Fig.17b. The data measured from AuAu reactions with two different detectors and other accessories have been shown separately and the other set of data is from PbPb collision. But the hydrodynamic model of Peitzmann is based on a version of this model of Weidemann and Heinz who includes transverse flow and resonance decays. Besides, Peitzmann also introduced the spatial distribution of Woods-Saxon type instead of simple Gaussian; reckoned with the difference between chemical freeze-out and kinetic freeze-out temperatures instead of one universal freeze-out temperature, and also the role of baryonic chemical potential. The certain degree of rigour in calculations is reflected in fair achievements in the collisions of the two heavies. But even with such physics considerations for actual calculations, the number of hand-inserted parameters are too large in the Peitzmann's latest model compared to just three in total in our approach. In our case the entire collective effects arising out of multiple nucleon-nucleon collisions and the effects of nuclear geometry are absorbed by the very simple term,  $(AB)^{g(p_T)}$ . And the rest depends on just the results of PP collisions. So, our approach is much straightforward compared to the existing other numerous complicated approaches of the models.

### 6. Summary and Outlook

What we have done here seems, by now, to be pretty clear. We have precisely introduced a simple parametrization of pion transverse momentum spectra for nucleus-nucleus collisions at high energies in terms of that for proton-proton collision at the same energy. Analyzing a large variety of colliding systems at different energies we have shown that the ratio of the two transverse momentum spectra approximately proportional to the product of the mass numbers of the colliding systems raised to a power that is a quadratic function of the transverse momentum of the particle under consideration. Furthermore, this quadratic function is essentially universal, i.e. its coefficients have only very weak dependence on the colliding systems and energies.

Through the massive demonstration of the fair agreements between measured data and our calculations the merit of the totality of the present approach is modestly well-made from the functional point of view. Despite this, let us sum up first here the important finer physical points which are the distinctive traits of the GCM alone. (i) Firstly, the GCM provides the most economical description of the vast body of experimental data on pion production in diverse set of reactions with only three arbitrary parameters. (ii) Secondly, the choice of the quadratic parametrizations for  $p_T$ -dependence of nuclear cross-sections is one of our important contributions. (iii) Thirdly, we have suggested independently an approach for computing the values of inclusive cross sections for production of pions in PP collision with the help of the plots on  $p_0$  vs.  $\sqrt{s}$  and n vs.  $\sqrt{s}$  at any high energy point of the c.m.energy values. (iv) Once the energy-dependence in PP collision is taken care of by this method, the inclusive cross sections for pion production in NA/AB interactions becomes essentially energy-independent. In other words, energy-dependence in nuclear collisions at high energy is manifested only through the very basic interacting sets of proton-proton collisions. No reflection of energy-dependence is detected in this mechanism in the nuclear geometry of collisions. This is in striking contrast with the most of the existing models. (v) We have also arrived at a sort of mass-number scaling of the parameters in the exponent of the nuclear dependent terms. This is also in sharp variance with the standard frameworks, though admittedly such a scenario is possible with only suitable adjustment of the normalization terms in the inclusive cross sections. (vi) Besides, we have tried to provide substantial support to the proposed connector here between NN and NA/AB reactions by making our studies as extensive as possible in order to impart a good degree of reliability to this combinational approach. (vii) Finally, this work brings out the features of 'universality' of all high energy particle and nuclear interactions in a satisfactory manner.

But the approach, despite its successes, suffers from the following gross limitations: (i) The master formula that is at the root of the success is not and cannot be derived right now from any of the first principles of basic physics. (ii) Data on production of a specific variety of particles in PP collisions at a few high energies are an indispensable necessity for analyzing and explaining the case of production of this particular particle species in

any nuclear collision. This PP-dependency is, by all indications, an inseparable part of this grand combination of models (GCM), though this might appear, at times, to be an intractable problem arising out of the lack of measured data on PP reaction at any particular energy. (iii) Thirdly and finally, the approach is totally insensitive to the physics of space-time-evolution of the collisions. But, seen from the angle of calculations on production of the final particles, this might be considered an advantage as well.

### References

- [1] McLerran L and Schuffner-Bielich J 2001 Phys. Lett. B 514 29.
- [2] Pirner H J and Yuang F 2001 Phys. Lett. B 512 297.
- [3] Adler C et al , STAR Collaboration 2001 Phys. Rev. Lett. 87 112303.
- [4] Wang E and Wang X 2001 Phys. Rev. C 64 034901.
- [5] Wong C Y 1986 Phys. Rev. D 33 711; Hao S B and Wong C Y 1985 Phys. Rev. D 32 1706.
- [6] Zhen B P and Ming S Y 1996 Phys. Lett. B 375 355.
- [7] De Bhaskar, Bhattacharyya S and Guptaroy P Int. Jour. Mod. Phys. A(to be published).
- [8] Hagedorn R 1965 Nuovo. Cim. Suppl. 3 147; ibid 1968 6 169.
- [9] Hagedorn R 1983 Riv. Nuovo. Cim. **6** 1.
- [10] Faessler M A 1984 Phys. Rep. 115 1.
- [11] Peitzmann T 1999 Phys. Lett. B 450 7.
- [12] Schmidt H R and Schukraft J 1993 J. Phys. G 19 1705.
- [13] Bielich J S et al 2002 Nucl. Phys. A 705 494.
- [14] Albrecht R et al , WA80 Collaboration 1998 Eur. Phys. Jour. C 5 255.
- [15] Antreasyan D et al 1979 Phys. Rev. **D** 19 764.
- [16] Aggarwal M M et al , WA98 Collaboration 2002 Eur. Phys. Jour. C 23 225.
- [17] David G, PHENIX Collaboration 2002 Nucl. Phys. A 698 227.
- [18] Adcox K et al , PHENIX Collaboration 2002 Phys. Rev. Lett. 88 022301.
- [19] Akesson T et al, NA34 Collaboration 1990 Z. Phys. C 46 369; Drees A, NA34 Collaboration, 1989 Ph.D. thesis, Heidelberg University, Germany.
- [20] Peitzmann T 2002 nucl-th/0207012.
- [21] Wang X N and Gyulassy M 1991 Phys. Rev. D 44, 3501; Wang X N 1997 Physics Reports 280 287.
- [22] Alper B et al 1975 Nucl. Phys. **B 100** 237.
- [23] Drijard D et al 1982 Nucl. Phys. B 208 1.
- [24] Albajar C et al 1990 Nucl. Phys. B 335 261.
- [25] Bocquet J et al 1996 Phys. Lett. **B 366** 434.
- [26] Abe F et al 1988 Phys. Rev. Lett. **61** 1819.
- [27] Albrecht R et al , WA80 Collaboration 1988 Z. Phys. C 38 97.
- [28] Abreu M C et al , NA38 Collaboration 1993 Z. Phys. C 55 365.
- [29] Angelis A L S et al , BCMOR Collaboration 1987 Phys. Lett. B 185 213.
- [30] Clark A G et al 1978 Nucl. Phys. **B 142** 189.
- [31] Akesson T et al , HELIOS Collaboration 1990 Z. Phys. C 46 361.
- [32] Alber T et al 1998 Eur. Phys. Jour. C 2 643.
- [33] Wlodarczyk Z Proc. of the xxiii ICRC, Invited, Rapporteur & Highlight Papers, (Calgary, Alberta, Canada, 19-30 July 1993) Ed. D A Leahy, R B Hicks and D Venkatesan, Singapore: World Scientific p 355.
- [34] Agakichiev G et al , CERES Collaboration 1998 Nucl. Phys. A 661 23c.
- [35] Donaldson G et al 1976 Phys. Rev. Lett. 36 1110.

# i) PP Collision:

Table 1: Fit Values of  $p_0$  and n for PP Collisions at different energies.

$\sqrt{s}_{NN}(GeV)$	Relevant collision-specifics	$C_1$	$p_0$	n	$\frac{\chi^2}{ndf}$	$p_0/n$
23 31 45 53 63	$\pi^-,$ $y_{cm} = 0,$ min. bias	$192 \pm 6$ $219 \pm 5$ $241 \pm 5$ $240 \pm 7$ $248 \pm 6$	$2.48 \pm 0.12$ $2.229 \pm 0.004$ $1.89 \pm 0.01$ $1.83 \pm 0.01$ $1.78 \pm 0.01$	$18.88 \pm 0.76$ $17.08 \pm 0.04$ $14.97 \pm 0.06$ $14.25 \pm 0.03$ $14.07 \pm 0.02$	1.539 1.157 1.352 2.72 1.621	0.131 0.130 0.126 0.128 0.127

# ii) $P\bar{P}$ Collision:

Table 2: Fit Values of  $p_0$  and n for  $P\bar{P}$  Collisions at different energies.

$\sqrt{s}_{NN}(GeV)$	Relevant collision-specifics	$C_1$	$p_0$	n	$\frac{\chi^2}{ndf}$	$p_0/n$
200	charged, $\eta_{cm} = 0$ , min. bias	$414 \pm 7$	$1.52 \pm 0.01$	$11.18 \pm 0.02$	1.614	0.136
500	charged, $\eta_{cm} = 0$ , min. bias	$327 \pm 7$	$1.51 \pm 0.05$	$9.84 \pm 0.03$	1.787	0.153
630	$(h^+ + h^-)$ , $-3.0 < \eta_{cm} < 3.0$ , min. bias	$302 \pm 5$	$1.49 \pm 0.01$	$9.41 \pm 0.01$	1.694	0.158
900	charged, $\eta_{cm} = 0$ , min. bias	$412 \pm 9$	$1.50 \pm 0.05$	$9.43 \pm 0.02$	1.61	0.159
1800	charged, $-1.0 < y_{cm} < 1.0$ , min. bias	$370\pm7$	$1.48 \pm 0.01$	$8.79 \pm 0.03$	1.694	0.168

Table 3: Numerical Values of the parameters:  $\alpha$  and  $\beta$  for different high energy collisions.

Collision	$E(\mathrm{GeV})$	Relevant collision-specifics	$C_3$	$\alpha$ (GeV/c) <sup>-1</sup>	$\beta$ (GeV/c) <sup>-1</sup>	$\chi^2/\mathrm{ndf}$	Fig. No.
		comsion-specifics		(Gev/c)	(GeV/C)		110.
P + D	400	$\pi^-$ , min. bias	$400 \pm 20$	$0.21 \pm 0.06$	$0.04 \pm 0.01$	0.005	4
P + Be	400	$\pi^-$ , min. bias	$1700 \pm 80$	$0.20 \pm 0.05$	$0.040 \pm 0.015$	0.008	4
P + Ti	400	$\pi^-$ , min. bias	$(4.5 \pm 0.5) \times 10^3$	$0.21 \pm 0.05$	$0.04 \pm 0.015$	0.002	4
P + W	200	$\pi^-$ , min. bias	$(3.8 \pm 0.5) \times 10^3$	$0.20 \pm 0.04$	$0.04 \pm 0.02$	1.624	4
P + W	300	$\pi^-$ , min. bias	$(4.7 \pm 0.3) \times 10^3$	$0.17 \pm 0.02$	$0.031 \pm 0.002$	1.15	4
P + W	400	$\pi^-$ , min. bias	$(9.4 \pm 0.6) \times 10^3$	$0.14 \pm 0.03$	$0.02 \pm 0.01$	0.013	4
P + Au	200	$\pi^0, 1.5 \le \eta \le 2.1, \text{ min. bias}$	$(1.7 \pm 0.2) \times 10^4$	$0.16 \pm 0.01$	$0.04 \pm 0.01$	0.570	4
P + U	200	$(\pi^+ + K^+), 3.0 < y < 3.9$	$(3.8 \pm 0.1) \times 10^4$	$0.20 \pm 0.02$	$0.032 \pm 0.004$	0.903	4
D + D	480A	$\pi^0,  y_{cm}  < 0.4$	$360 \pm 16$	$0.25 \pm 0.05$	$0.026 \pm 0.008$	1.438	5
D + D	1400A	$\pi^0$	$(24 \pm 4) \times 10^4$	$0.18 \pm 0.03$	$0.04 \pm 0.01$	1.627	5
D + D	1900A	$\pi^0$	$(28 \pm 4) \times 10^4$	$0.15 \pm 0.02$	$0.04 \pm 0.01$	1.627	5
D + Au	200A	$h^-, 2.0 < y < 3.0, \text{ central}$	$138 \pm 20$	$0.23 \pm 0.02$	$0.04 \pm 0.02$	1.720	8
$\alpha + \alpha$	480A	$\pi^0,  y_{cm}  < 0.4$	$624 \pm 50$	$0.27 \pm 0.02$	$0.026 \pm 0.002$	0.015	5
O + C	200A	$\pi^0, 1.5 \le \eta \le 2.1, \text{ min. bias}$	$(7 \pm 1) \times 10^3$	$0.13 \pm 0.02$	$0.07 \pm 0.02$	1.475	6
O + W	200A	negative particles,	$(1.3 \pm 0.4) \times 10^3$	$0.18 \pm 0.02$	$0.031 \pm 0.005$	1.220	6
		1.0 < y < 1.9, min. bias	,				
O + Au	200A	$\pi^0, 1.5 \le \eta \le 2.1, \text{ min. bias}$	$(9 \pm 1) \times 10^4$	$0.161 \pm 0.004$	$0.038 \pm 0.003$	0.030	6
O + Au	200A	$h^-, 2.0 < y < 3.0$ , central	$(1.2 \pm 0.2) \times 10^3$	$0.15 \pm 0.02$	$0.040 \pm 0.005$	1.562	8
O + U	200A	$(\pi^+ + K^+)$ , $3.0 < y < 3.9$	$(5.3 \pm 0.2) \times 10^5$	$0.180 \pm 0.002$	$0.036 \pm 0.002$	1.359	6
S + S	200A	$\pi^0$ , $2.1 < y < 2.9$ , min. bias	$(6.1 \pm 0.4) \times 10^4$	$0.18 \pm 0.01$	$0.046 \pm 0.002$	1.603	7
S + Ag	200A	$h^-, 2.0 < y < 3.0, \text{ central}$	$(1.4 \pm 0.1) \times 10^3$	$0.150 \pm 0.004$	$0.04 \pm 0.01$	1.790	8
S + W	200A	negative particles,	$(1.13 \pm 0.08) \times 10^3$	$0.17 \pm 0.03$	$0.031 \pm 0.005$	1.566	7
		1.0 < y < 1.9, min. bias	,				
S + Au	200A	$\pi^0$ , 2.1 < y < 2.9, min. bias	$(2.0 \pm 0.2) \times 10^5$	$0.19 \pm 0.02$	$0.039 \pm 0.005$	1.080	7
S + Pb	200A	negative particles,	$230 \pm 40$	$0.15 \pm 0.05$	$0.05 \pm 0.02$	2.646	8
		2 < y < 4, central					
S + U	200A	$(\pi^+ + K^+)$ , 3.0 < y < 3.9	$(9.0 \pm 0.5) \times 10^5$	$0.17 \pm 0.02$	$0.03 \pm 0.01$	0.433	7
Au + Au	8450A	$\pi^0$ , $ \eta  < 0.35$ , min. bias	$120 \pm 40$	$0.15 \pm 0.02$	$0.036 \pm 0.003$	0.449	9
Au + Au	8450A	$\pi^0,  \eta  < 0.35, \text{central}$	$500 \pm 30$	$0.145 \pm 0.008$	$0.036 \pm 0.002$	1.524	9
Au + Au	8450A	$\pi^0$ , $ \eta  < 0.35$ , peripheral	$27 \pm 7$	$0.14 \pm 0.02$	$0.036 \pm 0.002$	1.836	9
Pb + Nb	160A	$\pi^0$ , 2.3 < y < 3.0, min. bias	$(2.7 \pm 0.4) \times 10^5$	$0.17 \pm 0.02$	$0.036 \pm 0.004$	1.614	7
Pb + Au	160A	charged pions,	$1230 \pm 5$	$0.18 \pm 0.03$	$0.035 \pm 0.002$	1.822	8
		$2.1 < \eta < 2.6$ , central					-
Pb + Pb	160A	$\pi^0$ , 2.3 < y < 3.0, min. bias	$(9\pm1)\times10^5$	$0.16 \pm 0.03$	$0.03 \pm 0.01$	1.070	7

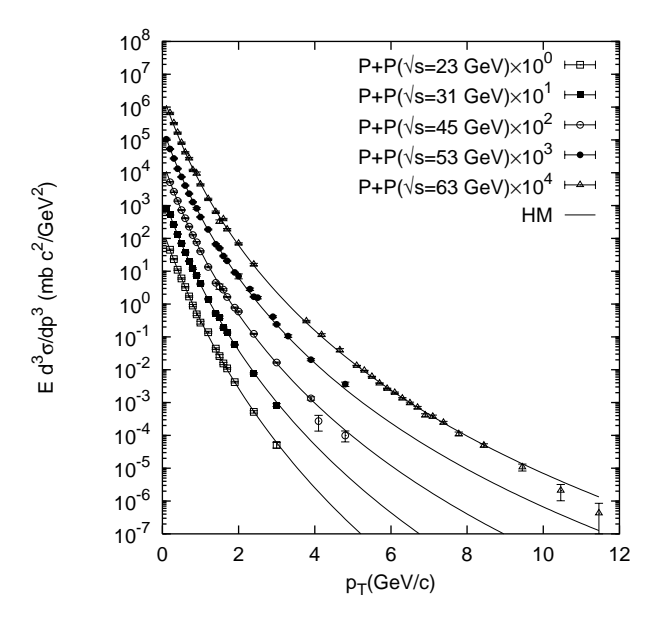


Figure 1: Plot of  $E\frac{d^3\sigma}{dp^3}$  vs.  $p_T$  for secondary pions produced in P+P collisions at different c.m. energies. The various experimental points are taken from Ref.[22] and Ref.[23]. The solid curves give the theoretical fits on the basis of Hagedorn's model(Eqn.3).

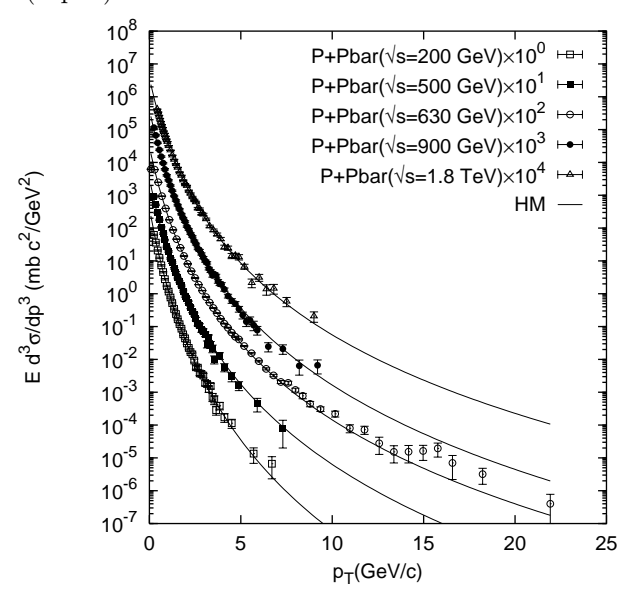


Figure 2: The inclusive spectra for secondary pions produced in  $P + \bar{P}$  collisions at  $\sqrt{s} = 200, 500, 630, 900$  and 1800 GeV. The various experimental points are from Ref.[24], Ref.[25] and Ref.[26]. The solid curvilinear lines are drawn on the basis of Eqn.3.

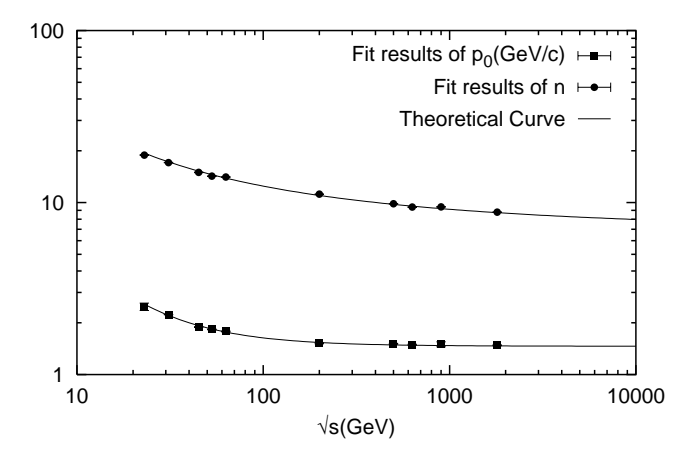


Figure 3: Values of  $p_0$  and n as a function of c.m. energy  $\sqrt{s}$ . Various data points are taken from Table-1 and Table-2. The solid curves are drawn on the basis of Eqn.4 and Eqn.5.

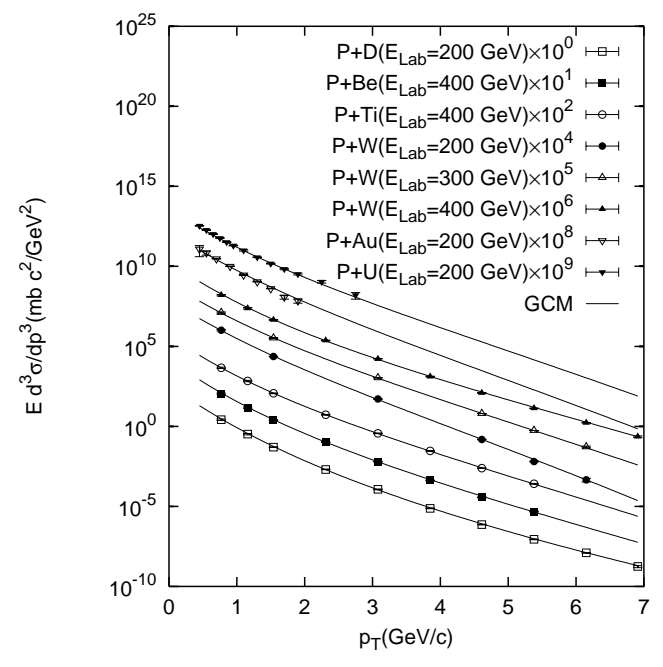


Figure 4: Plot of  $E\frac{d^3\sigma}{dp^3}$  for production of secondary pions in some Proton induced collisions at  $E_{Lab}=200,300$  and 400 GeV as a function of transverse momentum  $p_T$ . The various experimental data-points are taken from Ref.[15], Ref.[27] and Ref.[28]. The solid curves represent the fits on the basis of Eqn.8.

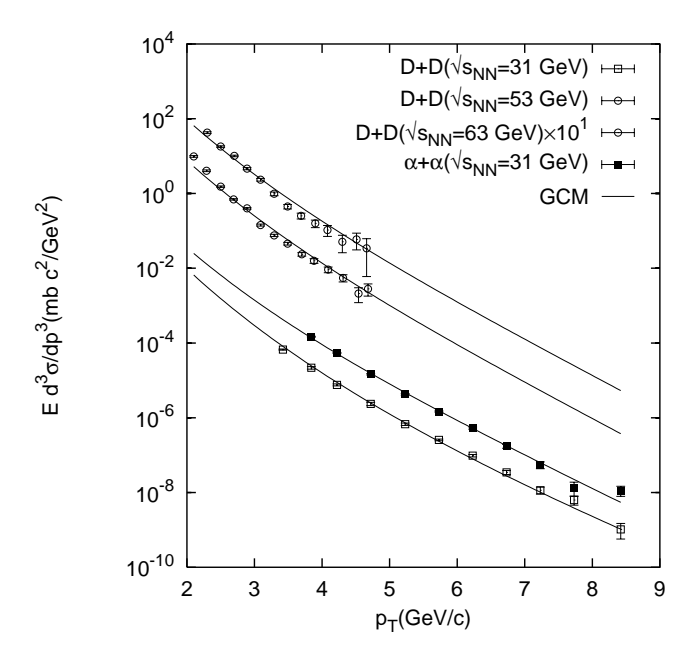


Figure 5: Plot of  $E\frac{d^3\sigma}{dp^3}$  vs.  $p_T$  for secondary pion produced in D+D and  $\alpha+\alpha$  collisions at different energies. The various experimental points are taken from Ref.[29] and Ref.[30]. The solid curves provide the fits on the basis of Eqn.8.

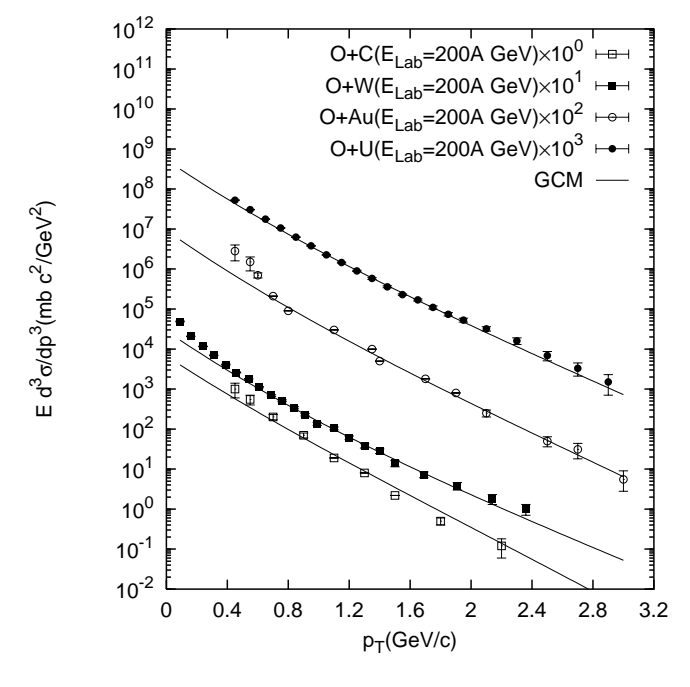


Figure 6: Nature of inclusive spectra for production of secondary pions in different Oxygen induced collisions at  $E_{Lab} = 200$ A GeV. The various experimental points are taken from Ref.[27], Ref.[28] and Ref.[31]. The solid curvilinear lines represent the fits on the basis of Eqn.8.

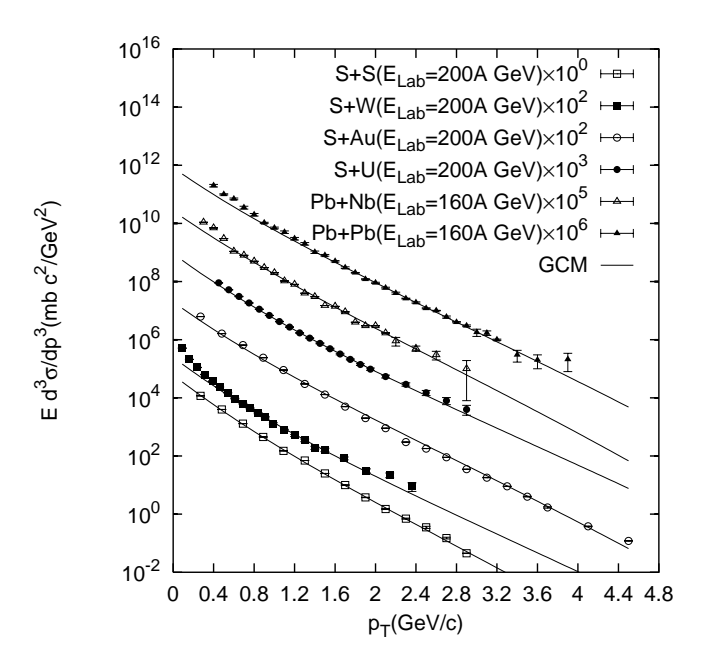


Figure 7: Plot of inclusive spectra vs.  $p_T$  for production of secondary pions in some sulphur-induced and lead-induced reactions at  $E_{Lab} = 200$ A GeV and at  $E_{Lab} = 160$ A. The various experimental data-points are from Ref.[14], Ref.[16], Ref.[28] and Ref.[31]. The solid curves provide the fits on the basis of Eqn.8.

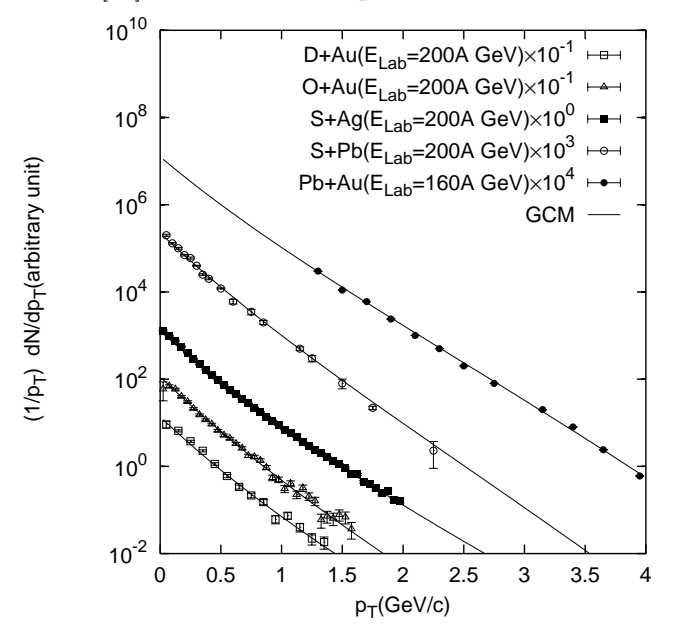


Figure 8: The nature of  $\frac{dN}{dp_T^2}$  for production of secondary pions in D+Au, O+Au, S+Ag and S+Pb collisions at  $E_{Lab}=200A$  GeV and in Pb+Au collision at  $E_{Lab}=160A$  GeV with change of transverse momentum. The various experimental points are taken from Ref.[32], Ref.[33] and [34]. The solid curves represent the fits on the basis of Eqn.8.

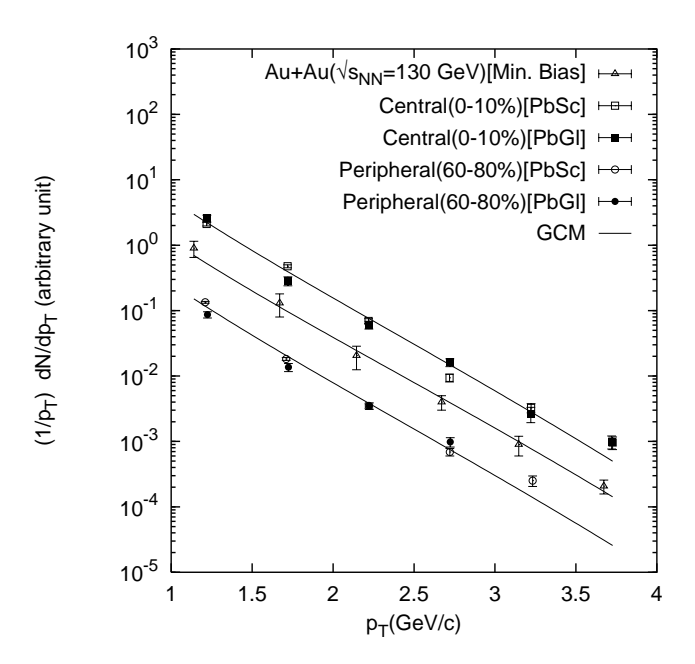


Figure 9: Invariant spectra for secondary pions produced in Au + Au reaction at  $\sqrt{s_{\rm NN}} = 130$  GeV(RHIC). The various experimental points are from Ref.[17] and Ref.[18]. Against the general background of pion production in Au + Au reaction, the symbols PbSc and PbGl indicate simply the two separate calorimeters; the former is the presentations of data-set obtained by lead-scintillator sampling calorimeter and the latter are those by lead-glass Cerenkov calorimeter. The solid curves give the fits on the basis of Eqn.8.

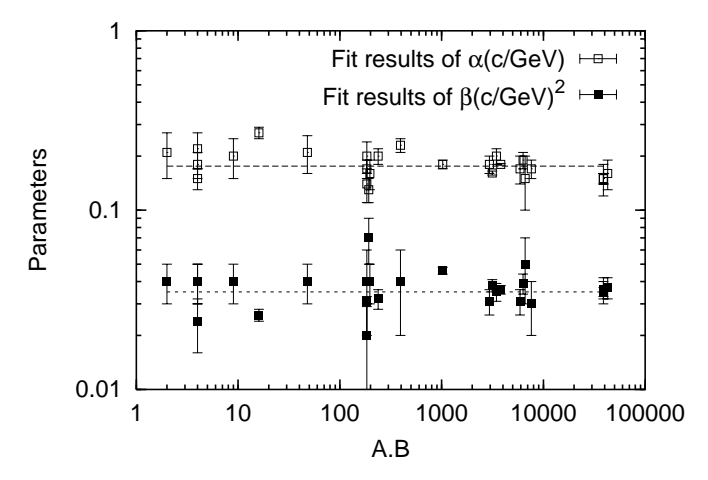


Figure 10: Values of  $\alpha$  and  $\beta$  for different collisions as functions of the product of mass numbers (AB) of the interacting nuclei. The fitted values of  $\alpha$  and  $\beta$ , enlisted in Table3, are taken as the data points; and are denoted by empty and filled squares respectively. The dashed line gives the average values  $0.18 \pm 0.03$  for  $\alpha$  and  $0.035 \pm 0.009$  for  $\beta$ .

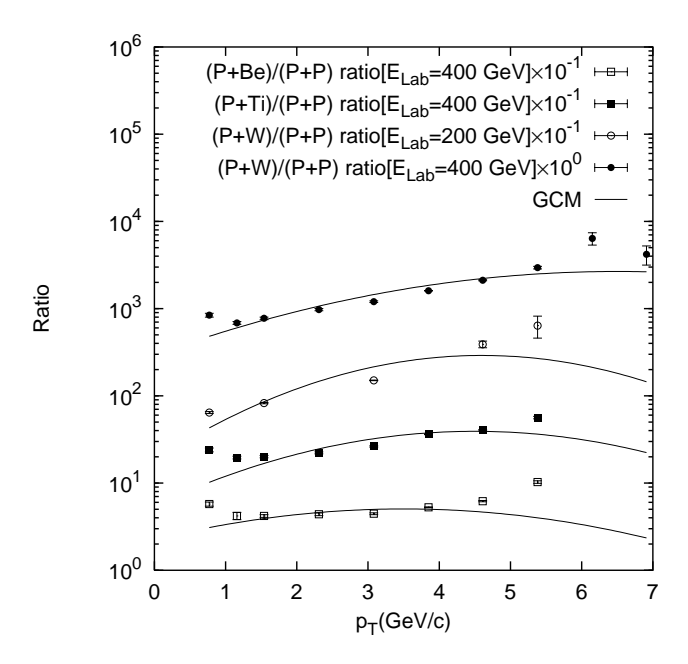


Figure 11: Plot of ratios of cross-sections for different Proton-induced collisions at different energies to that for Proton-Proton collisions at the corresponding energies. The data-points are taken from Ref.[15]. The present model-based results are shown by the solid curves.

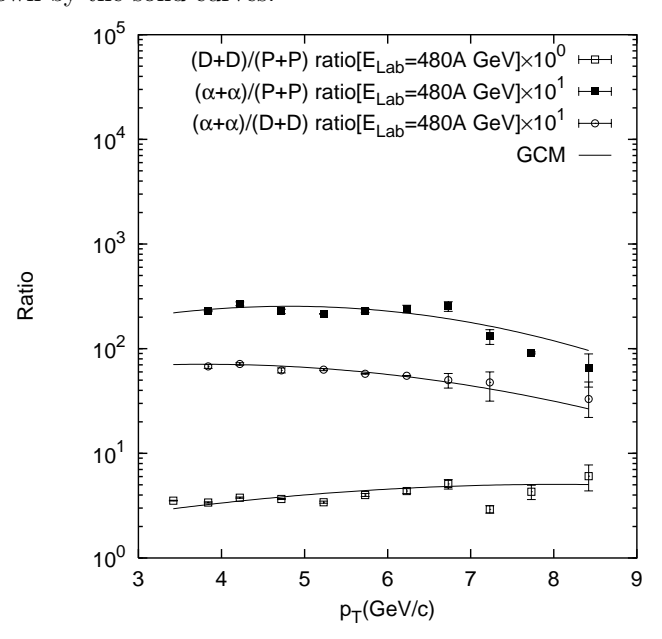


Figure 12: Plot of some cross section ratios as a function of  $p_T$ . The data points are taken from Ref.[29]. The solid curves depict the present model-based results.

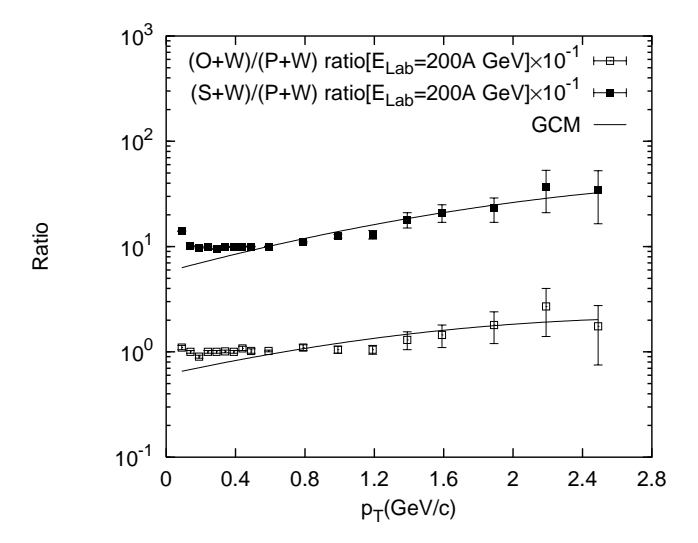


Figure 13: The nature of cross section ratios for  $\frac{O+W}{P+W}$  and  $\frac{S+W}{P+W}$  with respect to transverse momentum  $p_T$ . The data points are taken from Ref.[31, 35]. The present model-based results are shown by the solid curvilinear lines.

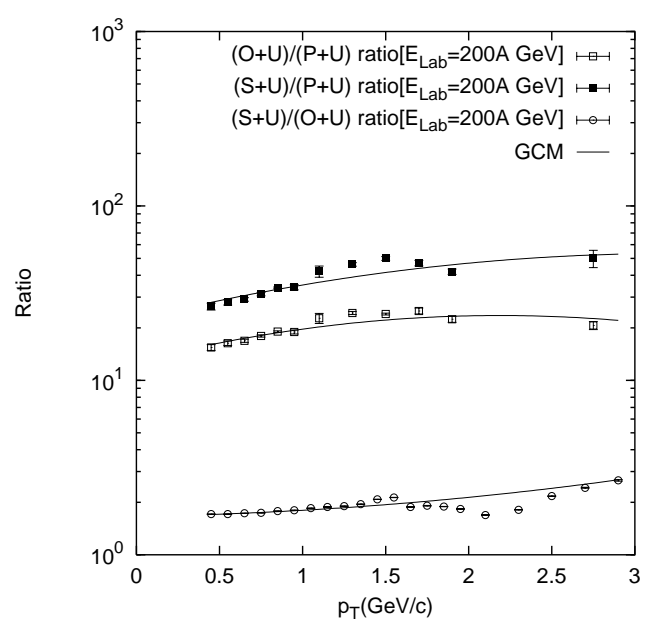


Figure 14: Plot of  $\frac{O+U}{P+U}$ ,  $\frac{S+U}{P+U}$  and  $\frac{S+U}{O+U}$  cross section ratios with respect to transverse momentum  $p_T$ . The data-points are taken from Ref.[28]. The solid curves provide the present model-based results.

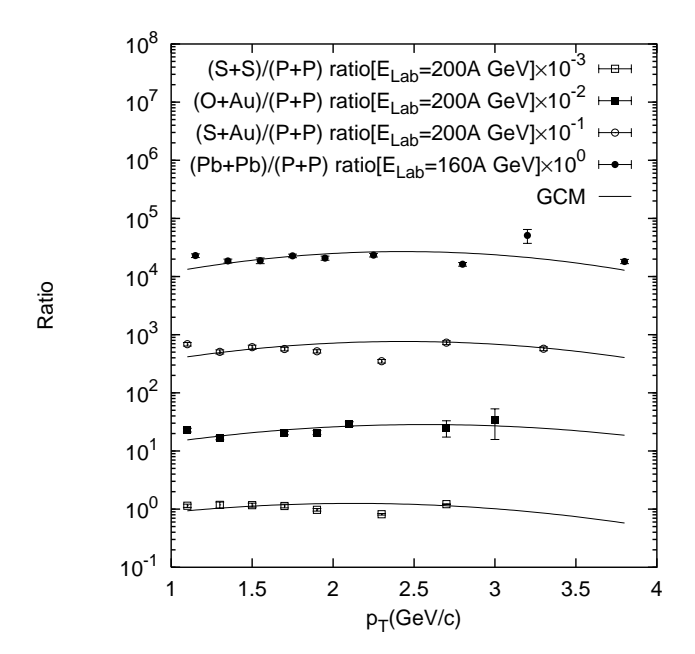


Figure 15: Plot of ratios of cross-sections for different Nucleus-Nucleus collisions at different energies to that for Proton-Proton collisions at the corresponding energies. The data points are taken from Ref.[14, 16, 27, 35]. To extract the  $\frac{Pb+Pb}{P+P}$  ratio-data, we have divided the data for Pb+Pb collision at 160A GeV by those for P+P collision at 200A GeV. And this is an approximation. The model-based results of the present work are shown by the solid curves.

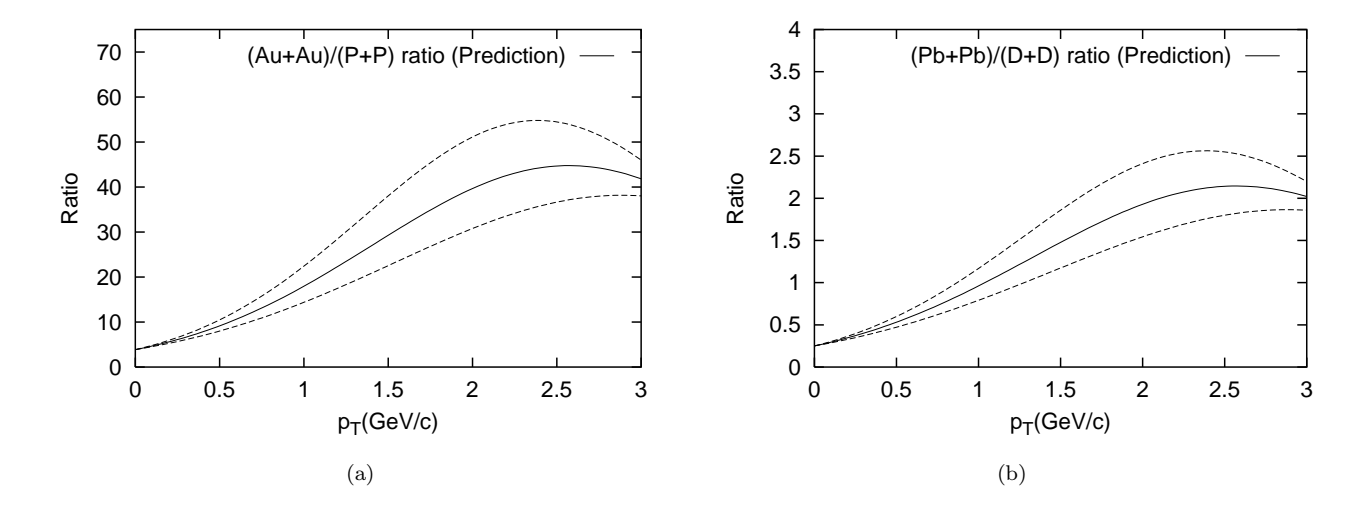


Figure 16: Predictive nature of  $\frac{Pb+Pb}{D+D}$  and  $\frac{Au+Au}{P+P}$  cross section ratio with respect to the transverse momentum $(p_T)$  on the basis of present model. The values of the ratio are certainly not exact, unless the  $\epsilon$ -value for pion production in corresponding reactions at any definite energy could be ascertained. The dotted curves depict the uncertainties arising out of the errors in  $\alpha$  and  $\beta$ .

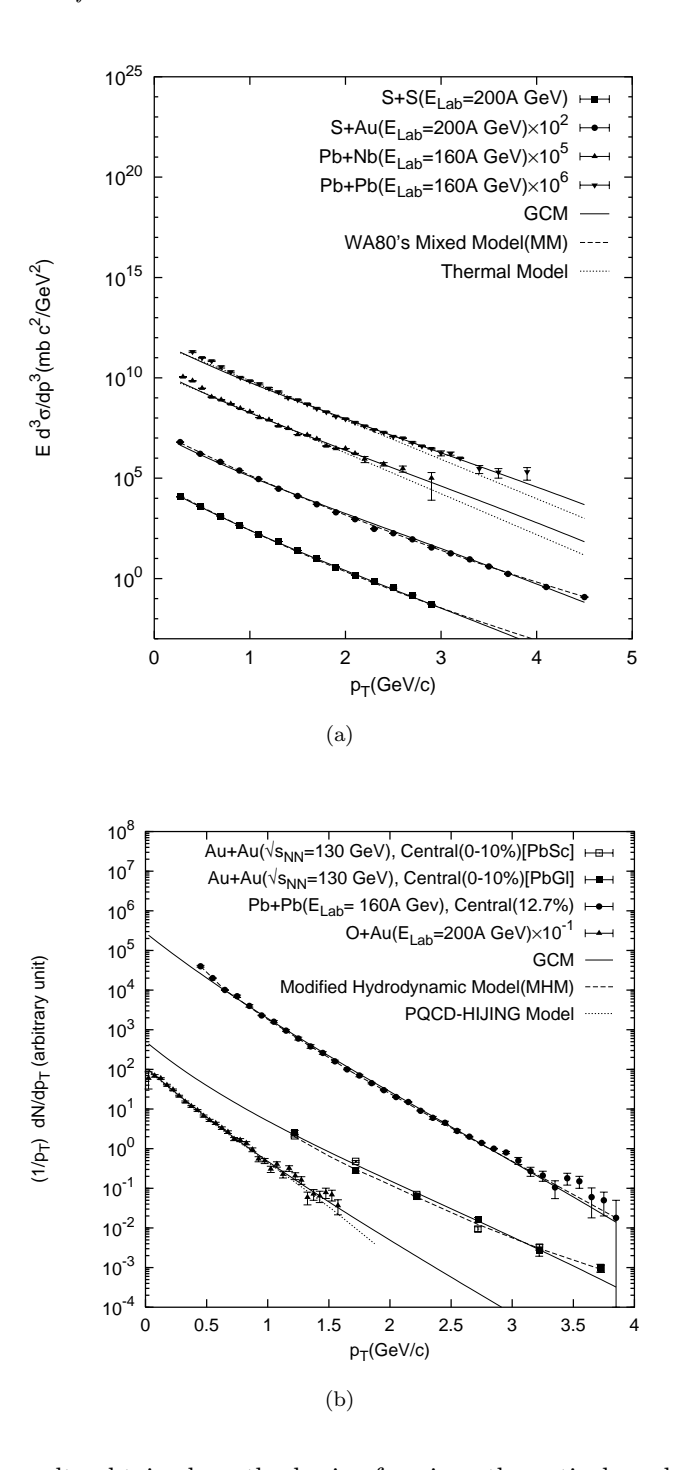


Figure 17: Comparison of results obtained on the basis of various theoretical models with those attained by GCM against measured data on pion production in some selected nucleus-nucleus collisions. For Fig.(17a) the data sources for SS and SAu, for PbPb and PbNb are [14] and [16] respectively. The theoretical plots based on Mixed Model and Thermal model are found from [14] and [16]. In Fig.17(b) the data on AuAu and PbPb are obtained from [18] and [16]. The source of the reports on measurements for OAu reaction is Ref.[32]. The theoretical plots based on MHM and on PQCD-HIJING model are assorted form [20] and [21].